Available online at www.sciencedirect.com
ScienceDirect
Journal of Nuclear Materials 374 (2008) 178–184
journal of nuclear materials
www.elsevier.com/locate/jnucmat

Microstructure and Charpy impact properties of 12–14Cr oxide dispersion-strengthened ferritic steels

Z. Oksiuta *, N. Baluc

Ecole Polytechnique Fédérale de Lausanne, Centre de Recherches en Physique des Plasmas, Association Euratom-Confédération Suisse, 5232 Villigen, PSI, Switzerland

Received 19 April 2007; accepted 9 August 2007

Abstract

This paper describes the microstructure and Charpy impact properties of 12–14 Cr ODS ferritic steels fabricated by mechanical alloying of pure Fe, Cr, W, Ti and Y_2O_3 powders in a Retsch ball mill in argon atmosphere, followed by hot isostatic pressing at 1100 °C under 200 MPa for 4 h and heat treatment at 850 °C for 1 h. Weak Charpy impact properties were obtained in the case of both types of as-hipped materials. In the case of 14Cr materials, the weak Charpy properties appeared related to a bimodal grain size distribution and a heterogeneous dislocation density between the coarse and fine grains. No changes in microstructure were evidenced after heat treatment at 850 °C. Significant improvement in the transition temperature and upper shelf energy of 12Cr materials was obtained by heat treatment at 850 °C for 1 h, which was attributed to the formation of smaller grains, homogenous in size and containing fewer dislocations, with respect to the as-hipped microstructure. This modified microstructure results in a good compromise between strength and Charpy impact properties.

1. Introduction

Ferritic steel is a term usually applied to a group of stainless steels with Cr contents in the range of 12–30 wt%. These steels are essentially ferritic in structure at all temperatures. Ferritic steels have a bcc structure and a microstructure mainly composed of dislocation cells, in comparison to the martensite laths encountered in martensitic steels [1]. Oxide dispersion strengthened (ODS) ferritic steels are usually obtained by introducing yttrium oxide (Y_2O_3) nano-particles in the aim of improving the creep strength and radiation resistance at elevated temperatures [2]. One of the possible routes to produce fine grained ODS ferritic steels is the consolidation of a mechanically alloyed (MA) powder by hot isostatic pressing (hipping). Hipping consists in the simultaneous application of heat and pressure and it is an excellent method to develop near-net-shape materials, to homogenise the composition of alloys and to close the micropores in cast alloys. It is also recommended as an alternative route to avoid strong anisotropy of materials as observed after hot extrusion (HE) for instance. As the result of hipping a dense material with very complex geometry can be obtained [3–8].

The main goal of this work is to investigate the influence of the consolidation parameters, annealing, chromium and titanium contents on the density, microstructure, microhardness and Charpy impact properties of reduced activation ODS ferritic steels that are candidate structural materials for application in fusion power reactors.

2. Experimental procedure

ODS ferritic steel powders with the chemical compositions given in Table 1 were prepared by MA elemental powders in a Retsch ball mill in argon atmosphere, followed by hipping. The parameters of milling were as follows: rotation speed = 300 rpm, ball-to-powder weight ratio (BPWR) = 8:1, milling time = 42 h.

* Corresponding author. Tel.: +41 56 310 2957; fax: +41 56 310 4529.
E-mail address: zbigniew.oksiuta@psi.ch (Z. Oksiuta).

0022-3115/$ - see front matter © 2007 Published by Elsevier B.V.
doi:10.1016/j.jnucmat.2007.08.004

Table 1
Chemical composition of Fe–(12–14)Cr–2W–0.3Ti–0.3Y_2O_3 ODS ferritic steels (in weight percent)

Material	C	Si	Cr	W	Ti	Mn	Mo	Y	O	N
12Cr	0.086	0.028	11.8	1.86	0.25	0.12	0.007	0.25	0.47	0.033
14Cr	0.088	0.031	13.7	1.84	0.26	0.16	0.008	0.23	0.48	0.035

After MA the powders were sealed, degassed, and closed in a stainless steel container under a vacuum of 10^{-2} Pa at 450 °C. Hipping experiments were performed in a SHIRP-2000 hipping device. Various hipping pressures in the range of 185–205 MPa and hipping times in the range of 3–5 h were investigated. The hipping temperature of 1100 °C was applied to avoid important coarsening of the nano-sized oxides. The cooling rate was 20 °C per minute. After hipping the ingots were heat-treated (HT) at 850 °C for 1 h in vacuum and furnace-cooled slowly to ambient temperature.

The microstructure of the specimens was investigated using scanning electron microscopy (SEM, Leo, Gemini 2000) equipped with an energy dispersive spectrometry (EDS) system, and transmission electron microscopy (TEM, Joel 2010). Samples for TEM were prepared by electrolytic thinning using a TENUPOL device. Vickers microhardness tests were performed at room temperature using a Vickers diamond pyramid (JENOPHOT 2000) and applying a load of 0.98 N for 15 s. Each result is the average of at least 20 measurements. The relative density of the specimens after hipping was measured by means of the Archimedes method using a laboratory analytical balance KERN ARJ 220-4M. Charpy impact tests were performed using an instrumented Charpy impact machine with an energy capacity of 30 J at temperatures ranging between −100 °C and 300 °C. V-notch KLST specimens ($3 \times 4 \times 27$ mm^3) for Charpy impact tests were machined parallel to the main axis of cylindrical ingots (20–22 mm in diameter, 27 mm in height). The ductile-to-brittle transition temperature (DBTT) was determined at the half-value of the upper shelf energy (USE) minus the lower shelf energy. Chemical analyses were performed using wavelength dispersive X-ray fluorescence spectroscopy (WD-XRF) as well as LECO TC-436 and LECO IR-412 analysers for detection of O, N and C contents, respectively.

3. Results and discussion

3.1. Powder consolidation

From results of chemical analyses of hipped ODS ferritic steel ingots, as reported in Table 1, it can be seen that these materials contain a high oxygen amount (about 0.48 wt%), which originates from the surface of powder particles and the MA atmosphere, and a relatively high carbon amount (about 0.087 wt%) that comes from the grinding media. Typical optical microscopy (OM) images of ODS ferritic steel ingots are shown in Fig. 1. The microstructure of the 14Cr ODS steel consists of a ferritic structure containing fine, equiaxed, prior particle boundaries (PPB), small pores and oxides (Fig. 1). The typical duplex (martensite plus α-ferrite) microstructure of the 12Cr material is observed. SEM observations of the ODS specimens revealed the presence of very fine, isolated pores, spherical in shape, that are decorated with the PPBs. The spherical shape of these voids suggests that they are gas micropores coming either from the oxygen layer of particles and/or from argon used in MA [9].

In general, a residual porosity was observed in all ODS ferritic steel ingots, even after hipping under a pressure of 205 MPa for 5 h. More than 99% of theoretical density (TD) was achieved when the specimens were consolidated under a pressure of 200 MPa for 3 h. Table 2 shows the influence of the hipping pressure on the density of the specimens. With increasing the hipping pressure the density of specimens also increases. However, no significant differences in density were measured for the specimens with different titanium contents.

TEM images of specimens of hipped Fe–(12–14)Cr–2W–0.3Ti–0.3Y_2O_3 ODS ferritic steels are presented in Figs. 2 and 3. After hipping, the microstructure of the 14Cr material consists of α-Fe matrix with two types of grains (Fig. 2(a)): small, about 500 nm in diameter, and coarse, about several μm in diameter, with oxide and

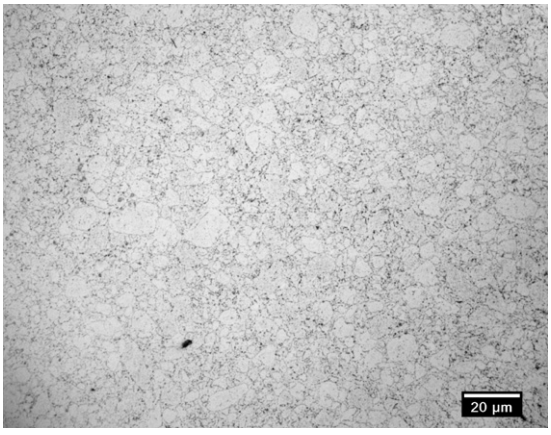

Fig. 1. OM image of the 14Cr–2W–0.3Ti–0.3Y_2O_3 ODS ferritic steel after hipping at 1100 °C under 200 MPa for 4 h.

Table 2
Effect of hipping pressure, at 1100 °C for 4 h, on the density of ingots of the ODS ferritic steel 14Cr–2W–0.3Ti–0.3Y_2O_3

Pressure (MPa)	185	195	205
Relative density (%)	95.8	98.2	99.5

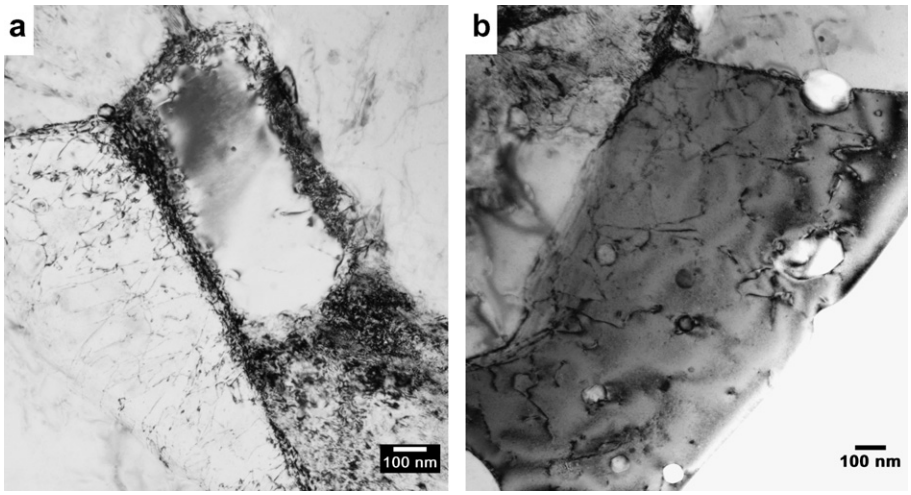

Fig. 2. TEM bright-field images of the as-hipped 14Cr–2W–0.3Ti–0.3Y_2O_3 material: (a) two types of grains and (b) oxides and carbides (precipitations).

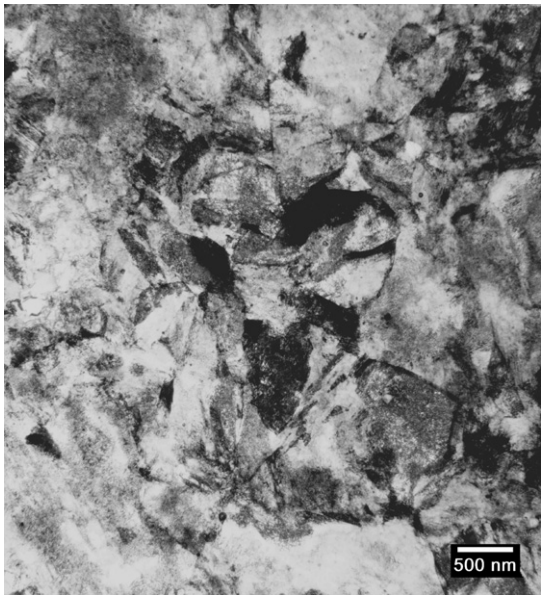

Fig. 3. TEM bright-field image of the as-hipped 12Cr–2W–0.3Ti–0.3Y_2O_3 material.

carbide impurities. The dislocation density in this material varies from dislocation-free areas to very dense dislocation tangles located especially at the fine grain boundaries. Moreover, TEM investigation revealed three different kinds of precipitates (Fig. 2(b)): oxide particles, about 100 nm in size, chromium carbides with an average size of about 50 nm and a chemical composition roughly analysed by EDS as 60Cr–25Fe–15W (wt%), and a high density of fine Y–Ti–O nano-clusters with a size in the range of 2–5 nm. After HT at 850 °C for 1 h no changes in the microstructure of the 14Cr ODS material have been observed.

The microstructure of the hipped 12Cr material consists of typical martensite laths (Fig. 3), despite the relatively low cooling rate. Some areas of α-Fe were also observed. Oxides and carbides, as well as spherical Y–Ti–O nano-clusters with a size in the range of 5–20 nm, are also present. The nano-clusters appear less homogeneously distributed and larger in size than in the 14Cr material. HT at 850 °C for 1 h yields the formation of tempered martensite made of smaller grains, homogeneous in size, a decrease of the density of dislocations and the formation of second phase precipitates (carbides) located inside the grains and at the grain boundaries (Fig. 4).

3.2. Microhardness measurements

Results of Vickers microhardness measurements are presented in Fig. 5. As they are related to the microstructure of the investigated material, it is easy to predict that the highest microhardness value after hipping should be obtained for the 12Cr materials, as confirmed by the value of 574

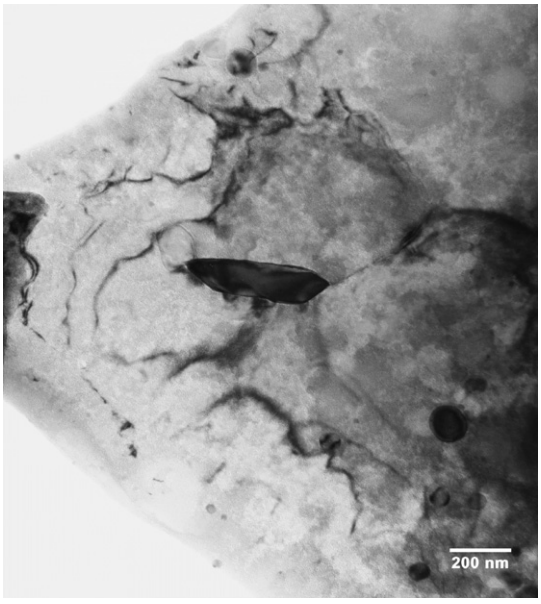

Fig. 4. TEM image of the 12Cr–2W–0.3Ti–0.3Y_2O_3 material after HT at 850 °C for 1 h.

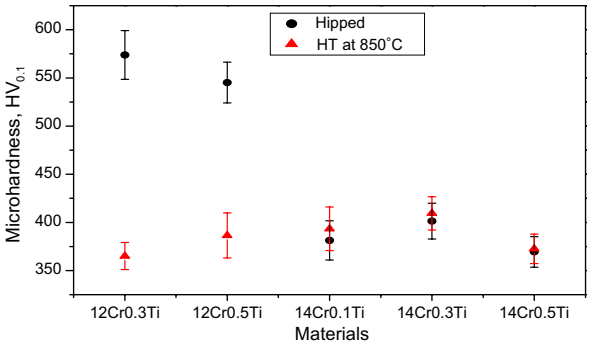

Fig. 5. Vickers microhardness of ODS ferritic steels after hipping and HT at 850 °C for 1 h.

$HV_{0.1}$ measured for the 12Cr–2W–0.3Ti–0.3Y_2O_3 material. An austenitization process takes place in 12Cr materials at the hipping temperature, and the austenite transforms into martensite during cooling. As reported by Mukhopadhyay et al. [10] a minimum Cr content of 13.5 wt% is required to get a fully ferritic structure. It seems that carbon, oxygen and nitrogen have also a strong influence on the stabilization of the γ-phase at the hipping temperature.

In agreement with the observed modifications of the microstructure of 12Cr materials after HT at 850 °C for 1 h, an important decrease in their microhardness is also observed after HT, indicative of a softening phenomenon. The higher microhardness value obtained after HT for the 12Cr0.5Ti material is probably due to the higher titanium content.

HT at 850 °C for 1 h has no significant impact on the microhardness of 14Cr materials, in agreement with the thermal stability of their microstructure. In addition, the titanium content has a minor influence on the microhardness of 14Cr materials.

3.3. Charpy impact tests and analysis of fracture surfaces

Charpy impact tests were performed on specimens of ODS ferritic steels with a density in the range 99.2–99.5% TD. Results of Charpy impact tests are reported in Figs. 6 and 7 and in Table 3. In general, all specimens were broken into two pieces in the full range of temperatures.

The 14Cr materials exhibit after hipping a very low USE and a high DBTT value (Fig. 6(a)). When the titanium content is increased from 0.1 to 0.5 wt%, the DBTT and USE slightly increase from 58 °C to 99 °C and from 1.3 J to 1.5 J, respectively. Heat treatment yields a significant increase in the DBTT of 14Cr0.1Ti materials, from 58 °C to 145 °C, while it seems to have a negligible influence on the DBTT and USE of other 14Cr materials (Fig. 6(b)). This may be attributed to the formation of smaller Y–Ti–O nano-clusters at higher titanium contents, which stabilize the microstructure during HT. However, it is difficult to draw a definitive conclusion, due to the very weak Charpy impact properties exhibited by these materials.

After hipping the 12Cr materials exhibit a very low USE of about 0.75 J (Fig. 7(a)). This is due to the features of the martensitic structure: martensite laths and high dislocation density. Therefore, 12Cr materials are high strength materials ($\sigma_0 > E/150$, σ_0 = yield strength, E = Young's modulus), as confirmed by the results of microhardness measurements (Fig. 5), with very low fracture toughness: brittle fracture occurs over a wide range of temperatures. A significant improvement in the impact properties of 12Cr0.3Ti materials is obtained after HT at 850 °C for 1 h. As shown in Fig. 7(b), after HT the DBTT is about 0 °C and the upper shelf energy is about 3.3 J. This improvement in impact properties is due to the microstructure of tempered martensite, which is made of equiaxed grains instead of martensite laths and contains a lower dislocation density than the original martensitic microstructure. In the case of the 12Cr0.5Ti material heat treatment results in a slight increase in the DBTT and USE values from 0 °C to 44 °C and from 0.75 J to 1.6 J, respectively.

SEM observations of the fracture surface of Charpy impact specimens showed that the fracture modes of 12Cr and 14Cr materials are similar. At testing temperatures corresponding to the lower shelf energy region (e.g.

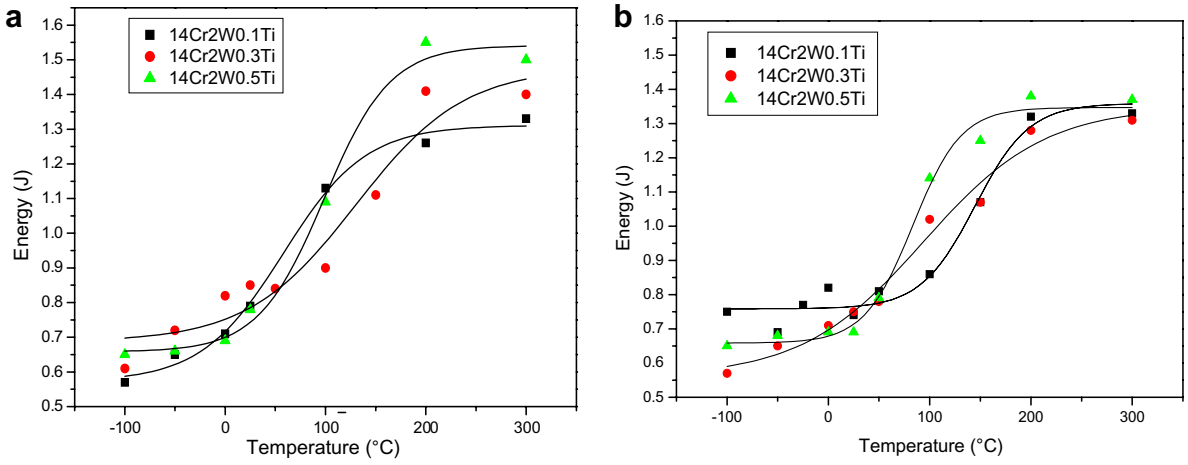

Fig. 6. Results of Charpy impact tests on 14Cr materials: (a) as-hipped and (b) after HT at 850 °C for 1 h.

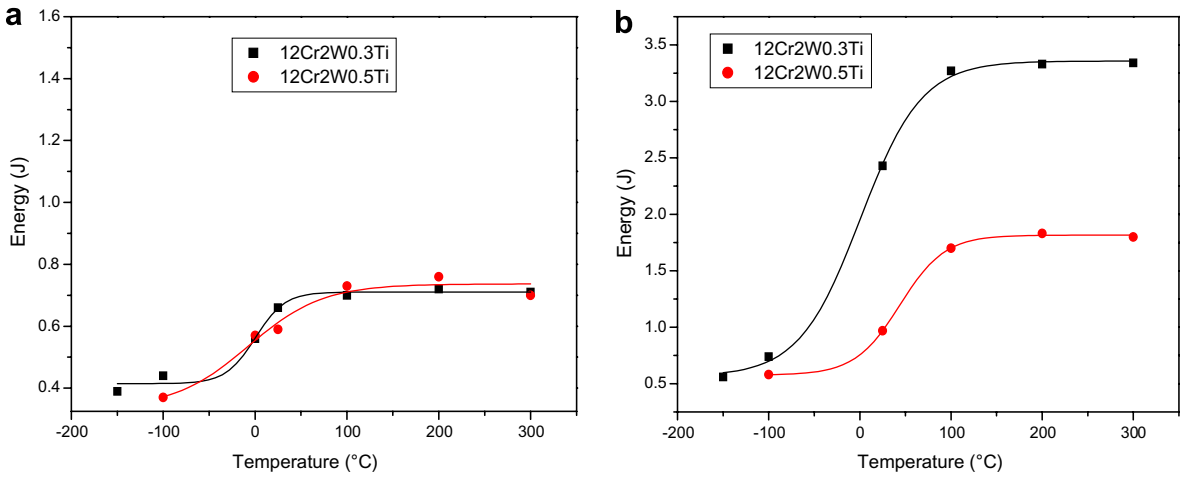

Fig. 7. Results of Charpy impact tests on 12Cr materials: (a) as hipped and (b) after HT at 850 °C for 1 h.

Table 3
Charpy impact properties before and after HT at 850 °C, 1 h, vacuum

Specimens	Before HT		After HT at 850 °C	
	USE (J)	DBTT (°C)	USE (J)	DBTT (°C)
14Cr–2W–0.1Ti	1.31	57.9	1.36	144.7
14Cr–2W–0.3Ti	1.47	121.6	1.35	93.9
14Cr–2W–0.5Ti	1.54	98.7	1.35	83.4
12Cr–2W–0.3Ti	0.71	0.3	3.36	0.7
12Cr–2W–0.5Ti	0.74	−7.2	1.82	43.8

−100 °C), river patterns can be seen, which are indicative of brittle fracture mode. Porosity and oxide inclusions are also observed, which are responsible for initiation of micro-cracks. Both cleavage and ductile fracture modes can be seen at testing temperatures corresponding to the DBTT region. At testing temperatures corresponding to the USE region (e.g. 200 °C), ductile microvoids are observed. However, singular cleavage facets are also visible. It appears that void nucleation and growth and cracking of specimens occur at the level of the pre-existing pores.

Fig. 8(a) and (b) show SEM images of fracture surfaces of heat-treated specimens of Fe–12Cr–2W–0.3Ti–0.3Y_2O_3 following Charpy impact testing at temperatures corresponding to the lower shelf energy region, the DBTT region, and the USE region, respectively. A transgranular, quasi-cleavage fracture mode is observed at temperatures corresponding to the lower shelf energy region (e.g. −100 °C) (Fig. 8(a)). As the grains are very small, it is difficult to determine the origin of cleavage cracks in this material. Both cleavage and ductile fracture modes are observed in the temperature range corresponding to the DBTT region (e.g. 0 °C). At 0 °C brittle fracture takes place near the notch of the specimens, due to three-dimensional stress conditions, while ductile fracture occurs in the remaining areas of the specimens. A typical example of ductile fracture at 200 °C is shown in Fig. 8(b). At low magnification, cups and cones are observed similar to the fracture features evidenced after uniaxial tensile tests.

On the basis of such observations it appears that the fracture mode of materials produced by powder metallurgy depends on porosity, oxide and carbide distributions, grain shape and size distribution and density of dislocations. In particular, the pores affect the fracture properties in the USE region where ductile failure of the specimens takes place. Oxygen increases significantly the DBTT. Carbon, which precipitates as carbides at the grain boundaries, promotes the propagation of cleavage cracks and decreases the USE. The grain size also influences the DBTT value [12].

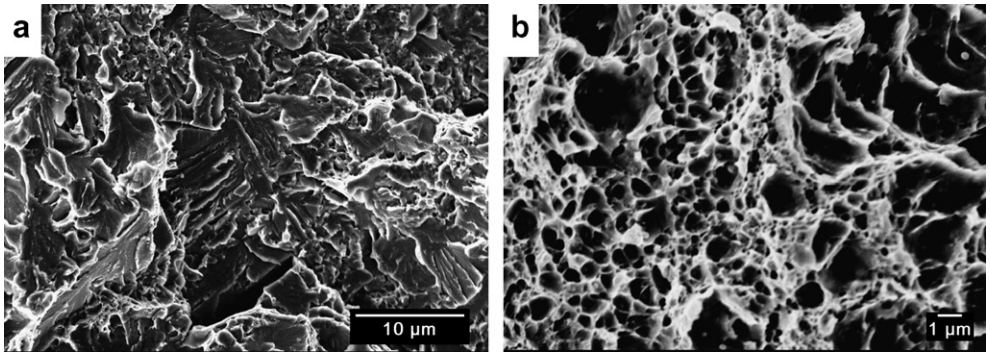

Fig. 8. SEM images of fracture surfaces of the heat-treated 12Cr–2W–0.3Ti–0.3Y_2O_3 material after Charpy impact testing at (a) −100 °C and (b) 200 °C.

The mechanism of stress concentration at the grain boundaries resulting from pile-ups of dislocations during deformation is well documented [11–13]. It is the probably worst situation when the microstructure consists of coarse grains surrounded by smaller sub-grains and/or by brittle precipitations, as it is observed in the case of 14Cr ODS ferritic steels (see Fig. 5(a)). This may lead to stress concentration, easy initiation of microcracks in the brittle particles, further crack propagation through the grains, and cleavage fracture over a wide range of temperatures [13]. On the contrary, the improvement in the Charpy impact behaviour of the 12Cr materials after HT seems to be due to the formation of a microstructure made of small, equiaxed grains, homogeneous in size, containing fewer dislocations than the original martensitic microstructure, made of martensite laths containing a high dislocation density, which results in a good compromise between strength and impact properties.

It is well known from the literature [2,14,15] that ODS ferritic or ferritic/martensitic steels are materials with high temperature strength but inferior impact properties (DBTT and USE) with respect to conventional ferritic or ferritic/martensitic alloys. Moreover, ODS steels possess a very low impact energy after hipping due to the existence of pores at the boundaries of sintered particles. However, forging or hot extrusion (HE) after hipping significantly improves the Charpy properties of these materials. This indicates that the USE and DBTT values of ODS steels strongly depend on the manufacturing conditions (microstructural state). It has been reported [16] that the MA957 ODS steel presents after HE very attractive DBTT and USE values of −100 °C and 7.7 J, respectively. After recrystallization, however, the DBTT increases up to 60 °C while the USE is increased by about 20%. The commercially available PM2000 ODS steel [17] has an USE twice higher (6.47 J at 300 °C) than that of the 12Cr ODS ferritic steel discussed in this work, but its DBTT is about two orders of magnitude higher (123 °C).

In general, the commercially available ODS ferritic steels exhibit at least twice higher USE values than the ODS materials presented in this paper but DBTT values are comparable. However, it is difficult to compare the impact properties of all ODS alloys due to the differences in chemical composition (different Cr, W, Ti, Y_2O_3 and O contents), manufacturing route (mechanical alloying, compaction) and parameters of final heat treatment. The data presented in this paper are preliminary results and more tests will be conducted in the aim to improve the fracture properties of 12–14Cr ODS ferritic steels.

4. Conclusions

The microstructure and mechanical properties of 12–14Cr ODS ferritic steels were examined after hipping and HT. The following general conclusions can be drawn from the obtained results:

1. More than 99% of theoretical density was achieved when the ODS ferritic steel powders were consolidated at 1100 °C under 200 MPa for 3 h.
2. Residual porosity was observed in all compacted ODS ferritic steel ingots, even after hipping at 1100 °C under 205 MPa for 5 h.
3. All ingots contain a high density of Y–Ti–O nano-clusters, with a size in the range of 2–5 nm in 14Cr materials and in the range of 5–20 nm in 12Cr materials.
4. Porosity, oxide and carbide distributions, grain shape and size distributions as well as density of dislocations strongly influence the Charpy impact properties of hipped materials.
5. Low impact properties were obtained in the case of 14Cr ODS ferritic steels due to bimodal grain size distribution and heterogeneous dislocation density between the coarse and fine grains. Coarse grains are almost dislocation-free, whereas fine sub-grains are surrounded by tangles of dislocations.
6. 14Cr ODS ferritic steels seem to be unaffected by HT at 850 °C for 1 h. No significant changes in microstructure, microhardness and Charpy properties were evidenced.
7. Significant improvement in the DBTT and USE of 12Cr ODS ferritic steels was obtained after HT at 850 °C for 1 h, which is attributed to the formation of smaller, equiaxed grains, homogeneous in size, containing fewer dislocations, with respect to the as-hipped microstructure made of martensite laths containing a high dislocation density. This modified microstructure yields a good compromise between strength and impact properties.

Acknowledgements

This work has been performed within the framework of the Integrated European Project 'ExtreMat' (contract NMP-CT-2004-500253) with financial support by the European Community. It only reflects the view of the authors, and the European Community is not liable for any use of the information contained therein. This work has been also supported by the European Communities under the contract of Association between EURATOM and Confédération Suisse, has been carried out within the framework of the European Fusion Development Agreement. The views and opinions expressed herein do not necessarily reflect those of the European Commission.

References

[1] R.L. Klueh, D.R. Harries, High-Chromium Ferritic and Martensitic Steels for Nuclear Applications, Printed by Bridgeport, NJ, 2001.
[2] S. Ukai, M. Fujiwara, J. Nucl. Mater. 307–311 (2002) 749.
[3] H.Y. Bor, C. Hsu, C.N. Wei, Mater. Chem. Phys. 84 (2004) 284.
[4] H. Skoglund, M. Knutson Wedel, B. Karlson, Intermetallics 12 (2004) 977.
[5] J.M. Gentzbittel, I. Chu, H. Burlet, J. Nucl. Mater. 307–311 (2002) 540.
[6] D.J. Bardos, Biomater. Med. Dev. 1 (1979) 73.
[7] M.A. Ashworth et al., Powder Metall. 3 (1999) 243.

[8] T. Hirose, K. Shiba, M. Ando, M. Eneoda, M. Akiba, Fusion Eng. Des. 81 (2006) 645.
[9] C. Suryanarayana, Prog. Mater. Sci. 46 (2001) 1.
[10] D.K. Mukhopadhyay, F.H. Froes, D.S. Gelles, J. Nucl. Mater. 258–263 (1998) 1209.
[11] G.E. Dieter, Mechanical Metallurgy, SI Metric Ed., McGraw-Hill Book Company, London, 1988.
[12] R.A. Philips, J.E. King, J.R. Moon, Powder Metall. 43 (2000) 43.
[13] Y. Li, Y. Zhang, B. Sun, J. Wang, Bull. Mater. Sci. 25 (2002) 361.
[14] R. Lindau, A. Möslang, M. Rieth, M. Klimiankou, E. Materna-Morris, A. Alamob, A.-A.F. Tavassoli, C. Cayron, A.-M. Lancha, P. Fernandez, N. Baluc, R. Schäublin, E. Diegele, G. Filacchioni, J.W. Rensman, B.v.d. Schaaf, E. Lucon, W. Diet, Fusion Eng. Des. 75–79 (2005) 989.
[15] V. de Castro, T. Leguey, A. Muñoz, M.A. Monge, P. Fernández, A.M. Lancha, R. Pareja, J. Nucl. Mater. 367–370 (2007) 196.
[16] A. Alamo, V. Lambard, X. Averty, M.H. Mathon, J. Nucl. Mater. 329–333 (2004) 333.
[17] G. Filacchioni, U. De Angelis, Tensile and impact properties of PM 2000, a commercial ODS ferritic steel, ENEA Technical Report MAT-CMS 006-002 (2002).